Kinetic Parameter Estimation for a Multiresponse Nonlinear Reaction Model

Kamalakanta Routray and Goutam Deo
Dept. of Chemical Engineering, Indian Institute of Technology Kanpur, Kanpur, India 208 016

DOI 10.1002/aic.10446
Published online April 21, 2005 in Wiley InterScience (www.interscience.wiley.com).

The kinetic parameters are successfully estimated for the propane oxidative dehydrogenation (ODH) reaction over vanadia–alumina catalyst under steady-state conditions. The 5% V_2O_5/Al_2O_3 catalyst is synthesized using an incipient-wetness impregnation technique. Characterization studies, such as surface area measurements, Raman spectroscopy, and temperature-programmed reduction (TPR), reveal that only reducible molecularly dispersed surface vanadium oxide species are present and the Al_2O_3 support is not affected. Reaction data suggest that CO_x's (CO and CO_2) are secondary products. Consequently, a single-site consecutive Mars–van Krevelen (MVK) mechanism is chosen to explain the reaction data. This consecutive reaction mechanism explains the steady-state reaction data obtained as a function of reaction temperature and propane to oxygen molar ratio. The kinetic parameters are estimated using a nonlinear multiresponse analysis. A determinant criterion is used as the objective function for minimization, which is achieved with a real-coded genetic algorithm (GA). Based on a profiling technique the kinetic parameters are tested for nonlinearity and correlation between parameters. Additional use of the profiling technique is in reparameterization and obtaining maximum likelihood intervals. The application of the estimated kinetic parameters for improved understanding of the reaction, the optimum conditions of reactor operation, and catalyst design are then discussed. © 2005 American Institute of Chemical Engineers *AIChE J,* 51: 1733–1746, 2005

Keywords: genetic algorithm, kinetic parameter estimation, multiresponse, profile plots, optimum condition, catalyst design

Introduction

Complex reaction networks are commonly encountered in the chemical process industry. These complex reaction networks are efficiently analyzed using kinetic modeling for better understanding of the reaction mechanisms. Kinetic parameter estimation is integral to the analysis of complex reaction networks. It is thus not surprising that kinetic parameter estimation is important in the design, optimization, and control of chemical processes.[1] The kinetic parameters obtained can also be effectively used for catalyst design. Ideally, the development of an efficient catalyst requires the combined knowledge from spectroscopic techniques and the kinetic parameters obtained from reaction studies. Combining information from these studies would assist in understanding the role of active sites in conjunction with the reaction mechanism. These studies will also assist in elucidating the reaction pathways at a microkinetic level. In the present study an attempt has been made to present the desired method of kinetic parameter estimation for complex reactions operating under steady-state conditions, especially for those that possess nonlinear reaction models.

Usually, reactions are carried out in a laboratory-scale reactor under steady-state and isothermal condition in a plug flow model to generate data for kinetic modeling or to study the activity and selectivity of a catalyst. It is desirable that the reactor used is properly designed,[2,3] such that a consistent,

Correspondence concerning this article should be addressed to G. Deo at goutam@iitk.ac.in.

accurate, and reliable data set is obtained. A proper data set makes the subsequent inferences trustworthy. Proper care should be taken to minimize transport limitations during the reactions because the quality of the data and subsequent estimation of kinetic parameters from it become spurious.[4]

Once the reactor has been suitably designed a proper data set can be obtained and the kinetic parameters can be estimated. To estimate kinetic parameters optimization of an objective function is required. A number of optimization techniques have been used in the literature to estimate the kinetic parameters. In addition to the traditional techniques such as Gauss–Newton[5] and Levenberg–Marquardt,[6,7] genetic algorithm (GA)[8,9] and Hybrid GA[6,7] have also been used in recent years for kinetic parameter estimations. The genetic algorithm uses the principle of natural evolution for search and optimization procedures.[10] It has gained popularity because of user-friendliness, robustness to a variety of problems, and its ability to converge to a global minimum.[11] In contrast, traditional convergence optimization techniques require good initial guesses to obtain optimized kinetic parameters, which otherwise might converge to local minima.[7] A reasonable initial guess should ideally remain near the global optima. This shortcoming of a good initial guess for traditional convergence optimization methods is obviated by the use of GA and Hybrid GAs, given that the initial guesses are randomly generated in the search space.

Unlike classical search and optimization methods, a GA begins its search with a random set of solutions, instead of a single solution. Each solution is evaluated by considering the objective function and associated constraints. After checking a termination criterion (taken here as $G_N > G_{Nm}$), three fundamental operators modify the population of solution and a new population set for the $(G_N + 1)$th generation is created. After GA operators create a new population set, the solution is evaluated in the context of the underlying objective function and constraint functions. In the absence of constraints, the fitness of a string is assigned an objective function value. The three operators required to facilitate the GA evolution cycle are relatively straightforward and simple. The fundamental operators are selection, crossover, and mutation. The selection operator provides the criteria for selecting solutions having the greatest fitness. The crossover operator recombines good substrings of two good strings together to form a better substring; and the mutation operator alters a string locally to create a better string.

For the proper estimation of kinetic parameters a suitable objective function is to be optimized. The choice of the objective function would depend on the type of analysis and system used. For example, in single-response systems the sum of squares is the desired objective function. However, for multiresponse systems, a determinant criterion, initially proposed by Box and Draper,[12] appears to be the objective function of choice. This determinant criterion considers the sum of squares and cross-products of the residuals. In some cases,[13,14] nonlinear least-square regression has also been applied for kinetic parameter estimation, although this method of analysis is not always suitable for multiresponse nonlinear systems.[12]

Kinetic parameter estimates obtained by fitting complex reaction models to data are often highly correlated with each other. For example, correlation among the Arrhenius parameters—preexponential factor and activation energy—is usually observed because of the large number of rate constants and their unknown magnitude range. Consequently, correlation among the parameters makes it difficult to determine reliable kinetic parameters. Under such circumstances the obtained kinetic parameters are of little use because they cannot correctly explain the actual nature of the reaction system. In this regard, a profiling technique proposed by Bates and Watts[15] is an excellent tool. Using the profiling technique correlations among the kinetic parameters can be ascertained. Additionally, profile plots are also applied to test the nonlinearity of a model and provide likelihood intervals. Thus, a proper estimation of kinetic parameters requires appropriate reactor-design, optimization technique, choice of objective function, and finally testing.

In the present study oxidative dehydrogenation (ODH) of propane over a well-characterized V_2O_5/Al_2O_3 catalyst has been chosen as an example for kinetic parameter estimation in nonlinear multiresponse reaction systems. Oxidative dehydrogenation has been suggested as a promising alternative for the production of high-value alkenes from alkanes. The ODH of alkanes to alkenes is a thermodynamically stable process because of the formation of water, which has a high enthalpy of formation. An added advantage of ODH lies in its irreversible nature. Because of the absence of equilibrium constraints it is theoretically possible to achieve complete conversion even at low temperature and high pressure. The presence of oxygen, however, enables side reactions such as CO and CO_2 formation to occur, thus reducing the selectivity to propane. Because the formation of carbon oxides is thermodynamically more favorable than the formation of olefins, it is necessary to intercept the desired products kinetically.[16] Furthermore, the use of a hydrocarbon–oxygen mixture increases the possibility of explosion. The lower and upper explosion limits of propane in air are 2.1 and 9.5%, respectively.[17] The kinetic parameters are estimated for the propane ODH reaction by minimizing a determinant. Minimization is achieved by using a genetic algorithm. The nonlinearity and correlation between the parameters is tested with the help of profile plots. The standard error and likelihood of the kinetic parameters are also calculated. Based on the kinetic parameters estimated and information from catalyst characterization reliable information about the catalyst-reaction system is obtained.

Experimental

Catalyst preparation and characterization

Catalyst Preparation. The catalyst was prepared by the incipient-wetness impregnation method using ammonium metavanadate (NH_4VO_3) as the precursor for the supported vanadium oxide phase. The γ-alumina support (Condea) was initially pretreated with an incipient volume of oxalic acid solution. The support was then dried at room temperature for 12 h, followed by drying at 383 K for 12 h, and finally calcined at 1273 K for 12 h. The support was washed several times with NH_4OH to clean the surface of any impurities that may arise from surface segregation at high temperature. Previous studies reveal that the surface of the alumina support is free from impurities.[18]

The incipient-wetness impregnation method of the above pretreated support was carried out with a vanadium oxalate solution, which was prepared by adding known amounts of ammonium metavanadate corresponding to 5 wt % V_2O_5, with

a stoichiometric amount of oxalic acid. The two were thoroughly stirred in doubly distilled water at 353 K until complete dissolution of the ammonia metavanadate solid was achieved. The deep blue solution formed was further diluted with doubly distilled water such that the total volume corresponded to the incipient-wetness impregnation volume of the support. The above solution was thoroughly mixed with the pretreated support in a crucible. The resulting paste was heat-treated similarly to the pretreatment of the support, except for the final calcinations, at 873 K. Thus, a 5% V_2O_5/Al_2O_3 sample was synthesized.

Catalyst Characterization. The 5% V_2O_5/Al_2O_3 sample was characterized by studying its surface area, Raman spectroscopy, and reduction characteristics. A Coulter SA 3100 apparatus was used for surface area analysis. The Raman spectrum was obtained under ambient condition using a Triplemate spectrometer (SPEX Model 1877) coupled to an optical multichannel analyzer (OMA III, Princeton Applied Research, Model 1463). The reduction profile was obtained in a Micromeritics Pulse Chemisorb 2705 analyzer. Details of the various instruments are given elsewhere.[18]

Genetic algorithm

The genetic algorithm used in the present study uses a real-coded fixed-boundary variable with tournament selection operator. The new strings are created by simulated binary crossover. The diversity in the strings is introduced by polynomial mutation. Finally, the fitness value of each string is estimated by using a proper objective function without any constraints. The terminating condition is then checked to see whether the required generation number is reached. Details about the source code of the program can be found elsewhere.[19]

Reaction studies

The ODH of propane was carried out in a fixed-bed, downflow, tubular quartz reactor at atmospheric pressure. The reactor was a single quartz piece with an inlet of 10 mm internal diameter and 150 mm long, and an outlet of 5 mm internal diameter and 150 mm long, to enable quick removal of the product gases. The two sections were tapered and fused. The catalyst bed was made from a physical mixture of catalyst and required amount of quartz powder to form a bed height of 1 cm and was placed just above the tapered region on quartz wool. The quartz particles helped reduce temperature hot spots, if any, along the catalyst bed. A PID (proportional–integral–derivative) controller (Fuji Micro controller X model PXZ-4) controlled the temperature of the catalyst bed within ± 1 K of the set point. The propane and air flow rates were adjusted by a separate electronic mass flow controller (Bronkhost Hi-Tech, El-flow Mass flow controller) such that the reactions can be carried out at different C_3H_8 to O_2 molar ratios for a specified total flow rate. The N_2 in air acted as the diluent to remove heat generated during the reaction. The product gases were sent for online analysis to a chromatograph (Aimil-Nucon 5765) equipped with a methanizer. The carbon oxides and hydrocarbons were analyzed in a flame ionization detector (FID) mode using a HYSEP Q column.

The reactor operation was vital for obtaining reliable data. The reactor used in this study was operated in steady-state, continuous plug-flow mode under isothermal condition and satisfied the following conditions:

(1) The diameter of the reactor was 10 times greater than the particle diameter to avoid channeling along its wall.[3]

(2) The Reynolds number ($\mathrm{Re} = d_p u/\nu$) was >30, which corresponded to a turbulent flow regime. Perfect mixing was ensured and the fixed bed reactor was best operated in this region.[2]

(3) Axial mixing effects on kinetics of any order were neglected by ensuring that z/d_p was >100.[2]

Transport resistances, if present, affect the reaction and may lead to spurious values of the kinetic parameters.[4] The transport limitations can be present at three levels: interphase, intraparticle, and interparticle. These limitations occur as a result of resistances between the solid catalyst and gas, within individual catalyst particles, and between the flow regions or catalyst particles, respectively. The absence of these transport limitations is tested by applying different criteria.[4,20]

Two data sets were obtained from the reactivity study: contact time data and data for kinetic parameter estimation. To study the effect of contact time on propane conversion and product selectivities, contact-time studies are carried out. A 2:1 C_3H_8 to O_2 molar ratio was maintained at 713 K and the total flow rate was varied from 30 to 105 cm^3/min with an increment of 15 cm^3/min.

To obtain the data set for kinetic parameter estimation the reaction data was obtained for a C_3H_8 to O_2 molar ratios of 1:1, 2:1, and 3:1, with a total flow rate of 50 cm^3/min. The temperature was varied from 673 to 733 K. Conversions were maintained $<10\%$ for all reactivity studies to ensure that mass and heat-transfer effects were absent in the reaction data. Blank experiments were performed to determine the homogeneous contributions to the net reaction. None was observed under the experimental conditions used in the present study.

Conversion, propene selectivity, propene yield, and carbon balance were calculated by using the following formulae

$$\text{Conversion (\%)} = \frac{\text{moles of propane converted}}{\text{moles of propane in}} \times 100 \quad (1)$$

$$\text{Propene selectivity (\%)} = \frac{\text{moles of propene formed}}{\text{moles of propane converted}} \times 100 \quad (2)$$

$$\text{Propene yield (\%)} = \frac{\text{moles of propene formed}}{\text{moles of propane in}} \times 100 \quad (3)$$

$$\text{C-balance} = \frac{\text{moles of carbon in products}}{\text{moles of carbon in reactant}} \quad (4)$$

Design equation

The most general mass equation for an integral, packed-bed reactor is given by the following equation[2]

$$\frac{\partial f}{\partial n} = \frac{1}{d_p u/D_r}\left(\frac{\partial^2 f}{\partial m^2} + \frac{1}{m}\frac{\partial f}{\partial m}\right) + \frac{1}{d_p u/D_r}\left(\frac{\partial^2 f}{\partial n^2}\right) + \frac{\sigma \sum R_v}{c_0 n} \quad (5)$$

where $f = c/c_0$, $n = z/d_p$, and $m = r/d_p$.

The term in the lefthand side represents the variation of concentration with length, whereas the 1st and 2nd terms in the right-hand side present the radial and axial concentration diffusion terms, respectively. The last term in the righthand side is the mass generated during the reaction.

The following assumptions are made to assist in modeling the reactor containing the catalyst.

(1) Reactor operates under isothermal and steady-state conditions.
(2) Fluid properties are independent of temperature.
(3) Pressure drop in the catalyst bed is negligible.
(4) Thermal conduction in catalyst particles is absent.
(5) Radial heat and concentration gradient are absent.
(6) Diffusion or mixing in the axial direction is negligible.
(7) Catalyst deactivation is within experimental limits.
(8) Gas-phase reactions are negligible.

After applying the above assumptions to Eq. 5, the reduced equation can be written as

$$\frac{df}{dn} = \frac{\sigma \sum R_v}{c_0 n} \Rightarrow \frac{dc}{dW} = \frac{\sum R_w}{F_T} \tag{6}$$

For a particular component i, Eq. 6 can be rewritten as

$$\Rightarrow \frac{dc_i}{dW} = \frac{\sum R_{wi}}{F_T} \tag{7}$$

For laboratory reactors using gases as reactants and assuming ideal gas conditions, it is beneficial to express the composition of the gas in Pa (pascal) rather than mol/cm^3. Consequently, Eq. 7 for gaseous reactant is modified as follows

$$\frac{dx_i}{dW} = \frac{\sigma \sum R_{pi}}{P_T} \tag{8}$$

The rate expression R_{pi} contains the unknown kinetic parameters in addition to the composition terms. Thus, the unknown kinetic parameters can be estimated by simultaneously solving the set of equations given by the following equation

$$\frac{dx_i}{dW} = \frac{\sigma \sum R_{pi}}{P_T} \tag{9}$$

where $W = [0, W]$ and $x_i = X_i$.

The set of ordinary differential equations given by Eq. 9 was solved to obtain the final mole fraction of each component based on the input mole fraction of the component x_{io}, the knowledge of rate expression R_{pi}, and the temperature and pressure of the reaction. The rate of reaction R_{pi} was dependent on the nonlinear kinetic parameters and on some or all mole fractions. A fourth-order Runge–Kutta–Gill technique was applied to determine the outlet concentrations of each component from their respective net rate expressions by integrating Eq. 9.

ODH reaction scheme

For the ODH of propane over the 5% V_2O_5/Al_2O_3 catalyst a generalized reaction network, as shown in Figure 1, is initially considered. Only the state of carbon is shown in this reaction

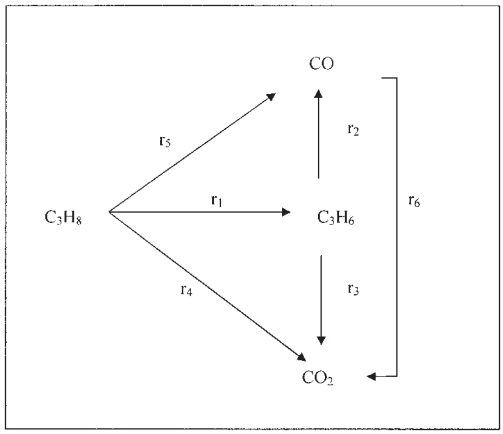

Figure 1. Generalized reaction scheme for propane ODH.

network scheme. According to the scheme the reaction of propane with oxygen can be presented in the form of six reactions steps, r_1 to r_6. Propene (C_3H_6) is formed by the ODH of propane (r_1), which can degrade to form CO and CO_2 by reactions r_2 and r_3, respectively. The carbon oxides, CO and CO_2, can also be formed directly from propane by reaction r_5 and r_4, respectively. Furthermore, CO_2 can be formed by the oxidation of CO by reaction r_6. Consequently, C_3H_6 is always a primary product, whereas CO can be a primary or secondary product; and CO_2 can be a primary, secondary, or tertiary product. Dehydrogenation (DH) of propane to propene is not considered because a DH reaction usually occurs at higher temperature. The stoichiometric equations corresponding to reactions r_1 to r_6 are given in the following series of equations

$$C_3H_8 + 0.5O_2 \rightarrow C_3H_6 + H_2O \tag{10}$$

$$C_3H_6 + 3O_2 \rightarrow 3CO + 3H_2O \tag{11}$$

$$C_3H_6 + 4.5O_2 \rightarrow 3CO_2 + 3H_2O \tag{12}$$

$$C_3H_8 + 5O_2 \rightarrow 3CO_2 + 4H_2O \tag{13}$$

$$C_3H_8 + 3.5O_2 \rightarrow 3CO + 4H_2O \tag{14}$$

$$CO + 0.5O_2 \rightarrow CO_2 \tag{15}$$

Among all the mechanisms proposed for propane ODH, the Mars–van Krevelen (MVK) model[13,14,21,23,24] has been widely accepted as the ideal model for propane ODH reaction. An MVK model considering carbon oxides as secondary products is used in the present study. The formation of carbon oxides as secondary products is consistent with previous studies, given that the formation of carbon oxides as primary products is small.[25] According to the MVK mechanism proposed for oxidative dehydrogenation reactions the alkane molecules react with lattice oxygen of the catalyst to produce alkene molecules. The gas-phase alkene molecules react with lattice oxygen forming carbon oxides as secondary products. Finally, the gas-phase oxygen replenishes the lattice oxygen by the reoxi-

dation of the catalyst. In the present study the carbon oxides (CO and CO_2) are represented as CO_x. Furthermore, the ratio between the numbers of moles of CO_2 to CO is represented by Ψ. The three reactions, r_1, r_2, and r_3, considered are given below.

(1) Formation of propene (r_1): The gas-phase propane reacts with lattice oxygen forming gas-phase propene

$$C_3H_8(g) + O(s) \rightarrow C_3H_6(g) + H_2O + *_{red} \quad (16)$$

where $*_{red}$ is a reduced site.

(2) Formation of CO_x from propene (r_2): The gas-phase propene reacts with lattice oxygen to form gas-phase CO

$$C_3H_6(g) + 3(\varepsilon + 1)O(s) \rightarrow 3CO_\varepsilon(g) + 3H_2O + 3(\varepsilon + 1)*_{red} \quad (17)$$

where ε is 1 for CO and 2 for CO_2.

(3) Reoxidation (r_3): Finally, the catalyst is reoxidized by gas-phase oxygen

$$O_2(g) + 2*_{red} \rightarrow 2O(s) \quad (18)$$

Rate expressions for the above three reactions (Eqs. 16–18) are

$$r_1 = k_1 P_{C_3H_8}(1 - \beta) \quad (19)$$

$$r_2 = k_2 P_{C_3H_6}(1 - \beta) \quad (20)$$

$$r_3 = k_3 P_{O_2}\beta \quad (21)$$

The rate constants k_i can be further simplified according to the Arrhenius expression; however, high correlations are frequently encountered between kinetic parameters in the Arrhenius expression for a rate reaction. Consequently, elucidation of the reaction network becomes very difficult.[26,27] Under such circumstances the spurious kinetic parameters do not predict the real nature of the reaction system. To reduce correlation the rate constants k_i are expressed in the modified Arrhenius form[28] as

$$k_i = k_{i0}\exp\left[-\frac{E_i}{R}\left(\frac{1}{T} - \frac{1}{T_m}\right)\right] \quad (22)$$

The inverse temperature is centered about the mean temperature range ($1/T_m$) of the reaction. This centering procedure eases the kinetic parameter search by minimizing the statistical correlation between activation energy and preexponential factor.[29]

The degree of reduction (β) is calculated as

$$\beta = \frac{0.5k_1P_{C_3H_8} + \frac{3(3\psi + 2)}{2(\psi + 1)}k_2P_{C_3H_6}}{0.5k_1P_{C_3H_8} + \frac{3(3\psi + 2)}{2(\psi + 1)}k_2P_{C_3H_6} + k_3P_{O_2}} \quad (23)$$

Thus, the gas-phase propane reacts with lattice oxygen to form propene (Eq. 19) with a rate constant k_1. Propene is further oxidized to CO_x (Eq. 20) with a rate constant k_2. Reoxidation (Eq. 21) of the reduced sites occur with a rate constant k_3. Consequently, there are six kinetic parameters in total that need to be estimated; a k_{i0} and E_i associated with each k_i.

Kinetic parameter estimation

In the present study propane (C_3H_8), propene (C_3H_6), carbon dioxide (CO_2), and carbon monooxide (CO) are simultaneously measured at each of the reaction conditions. Consequently, the present study is an exemplar of a multiresponse system. Furthermore, because the kinetic parameters are nonlinear their estimation requires the solution of multiresponse nonlinear systems.

The reaction data are modeled by the following nonlinear equation

$$y_{ui} = g_i(X_u, \theta) + z_{ui} \qquad u = 1, 2, \ldots, n \quad \text{and } i = 1, 2, \ldots, r \quad (24)$$

To estimate the kinetic parameters for a nonlinear multiresponse system given above, a suitable estimation criterion for the system dealing with more than one response needs to be developed. This situation arises for complex reactions where a number of rate or exit concentrations are simultaneously measured as in the present study. A consideration of all the responses in the estimation criteria is expected to provide a better set of kinetic parameters than considering only an important rate or exit concentration.

In some cases nonlinear least-square analysis is used as the estimation criterion and is given by

$$\sum_{i=1}^{r}\sum_{u=1}^{n}[y_{ui} - g_i(X_u, \theta)]^2 \overset{\theta}{\rightarrow} \min \quad (25)$$

The above criterion, however, is applicable only to cases where: (1) the responses are normally distributed, (2) the variance is identical for all experimental conditions, and (3) the responses are statistically independent.[30] In the event of violation of any of the above conditions, a determinant proposed by Box and Draper[12] should be used as the estimation criterion for kinetic parameter estimation. In the present study a determinant of a matrix $|\mathbf{Z^TZ}|$, proposed by Box and Draper,[12] is considered as the estimation criterion.[3,15,31-37] The determinant is represented by $Z(\theta) = \mathbf{Y} - G(\theta)$. For proper application of the determinant criterion, the number of multiresponse experiments should always be greater than or equal to the number of responses. A violation of the restriction makes the $|\mathbf{Z^TZ}|$ identically zero. It is also required that the number of experiments should be greater than the number of kinetic parameters to be calculated from the given model.[28,38] While using the determinant matrix for kinetic parameter estimation special care should be taken because a singular determinant matrix is sometimes obtained.[39] A singular determinant matrix occurs because of a linear relation among data and/or among expected responses. Different ways of dealing with a singular $\mathbf{Z}$ matrix are described elsewhere.[28,32,39,40]

Table 1. Comparison between the Standard Error Obtained by Bates and Kang and the Present Study

Parameter	Standard Error	
	Kang and Bates[34]	Present Study
θ_1	0.036019	0.038957
θ_2	0.086922	0.084867

Standard error calculation

The standard error involved in the kinetic parameter estimation is important. Bates and Watts[40] approximated $d(\theta)$, the determinant $|\mathbf{Z^T Z}|$, by a quadratic Taylor series near $\hat{\theta}$ and presented the posterior density as

$$p(\theta|\mathbf{Y}) \propto \left[1 + \frac{(\theta - \hat{\theta})^T \mathbf{\Gamma} (\theta - \hat{\theta})}{2|\mathbf{Z^T Z}|}\right]^{-N/2} \tag{26}$$

The $\hat{Z}$ and $\mathbf{\Gamma}$, the Hessian matrix of $d(\hat{\theta})$, are evaluated at the kinetic parameter values $\hat{\theta}$. The covariance matrix of $\hat{\theta}$ is $2s^2\mathbf{\Gamma}^{-1}$, where $s^2 = d(\hat{\theta})/(N - P)$ and is evaluated by dividing the optimized determinant value by the degrees of freedom $(N - P)$. The standard error $se(\hat{\theta}_p)$ for the kinetic parameters θ_p is then given by $se(\hat{\theta}_p) = [(2s^2\mathbf{\Gamma}^{-1})_{pp}]^{0.5}$. In the present study a finite-difference method is used to calculate the Hessian matrix at $\hat{\theta}$. This finite-difference method has been applied with reasonable accuracy to the Box and Draper[12] data set and the standard errors are presented in Table 1 along with the standard errors calculated by Kang and Bates.[34] Kang and Bates[34] used a Gauss–Newton method for optimizing $d(\theta)$ by explicitly deriving the gradient and Hessian of $d(\theta)$. Comparison of the standard error values suggests the method used in this study is acceptable.

Profile plot

One of the simpler approaches of kinetic parameters estimation is based on the linear approximation of the nonlinear model. Although this method is quick and easy, ideally, the extent of nonlinearity of the model needs to be tested. Bates and Watts[15] developed a technique known as *profiling* to indicate the degree of nonlinearity of a model. This profiling tool is also useful for analyzing the correlation between parameters, further reparameterization, if any, required, and for developing likelihood intervals for nonlinear model kinetic parameters. In the profiling technique, the parameters θ are presented as (θ_P, θ_{-P}), where θ_{-P} is a vector of $(P - 1)$ parameters excluding the parameter θ_P. The profile t function for θ_P is defined as

$$\tau(\theta_P) = \text{sgn}(\theta_P - \hat{\theta}_P) \frac{\sqrt{\tilde{S}(\theta_P) - S(\tilde{\theta})}}{s}$$

and

$$\delta(\theta_P) = \frac{\theta_P - \hat{\theta}_P}{se(\hat{\theta}_P)}$$

The $\tilde{S}(\theta_P)$, known as the *profile sum of square*, is estimated at the point $[\theta_P, \tilde{\theta}(\theta_P)]$. The vector of points $\tilde{\theta}(\theta_P) = [\tilde{\theta}_1(\theta_P), \tilde{\theta}_2(\theta_P), \ldots, \tilde{\theta}_{P-1}(\theta_P), \tilde{\theta}_{P+1}(\theta_P), \ldots, \tilde{\theta}_P(\theta_P)]^T$ is known as the trace vector.

The profile t plot of $\tau(\theta_P)$ vs. $\delta(\theta_P)$ provides information about the nonlinear behavior of the parameter.[29] For a linear model, the profile t plot is a straight line passing through origin with a unit slope. Thus, deviation of a profile t plot from the 45 ° line indicates the nonlinearity of the kinetic parameter and the curvature of the plot reveals the extent of nonlinearity. Consequently, the information provided by the profile t plot for all the parameters should be judiciously used before making linear approximation. The nature of a profile t plot, for a particular parameter, also gives information about the further reparameterization required for that parameter.

By analogy with the profile t function described for least-square estimation criteria used for a single-response system, in the present case a different profile t function for θ_P, applicable to the determinant estimation criterion, is defined as[15,38]

$$\tau(\theta_P) = \text{sgn}(\theta_P - \hat{\theta}_P) \frac{\sqrt{\tilde{d}(\theta_P) - d(\tilde{\theta})}}{s}$$

The profile plots can also be used for producing an exact likelihood interval for nonlinear model parameters. A horizontal line is drawn through $\tau(\theta_P) = \pm t(N - P; \alpha/2)$ point on the vertical τ scale. The intersection point between the horizontal line and the profile t curve is reflected on the horizontal axis from which the exact likelihood intervals are obtained.

The pairwise plots of the trace vector vs. the profile parameter provide useful information. The plots of $\tilde{\delta}(\theta_q)$ vs. $\delta(\theta_p)$ and $\tilde{\delta}(\theta_p)$ vs. $\delta(\theta_q)$ are combined to generate the pairwise profile traces. From the profile traces any valuable information about correlation between parameters can be obtained. For a linear model the trace plot will be a straight line passing through the origin, with a slope representing the correlation between the parameters. Similarly for a nonlinear model the trace plot will be curved and the extent of deviation from a straight line reveals the degree of nonlinearity.

Results and Discussion

Characterization studies

The surface areas of the Al_2O_3 support and 5% V_2O_5/Al_2O_3 catalyst were determined to be 120 m^2/g. The similar surface area values for both samples suggest that the support structure is not affected. The 5% V_2O_5/Al_2O_3 catalyst was further characterized by Raman spectroscopy and H_2-TPR. The Raman spectra of the sample obtained under ambient conditions reveal a broad features at about 960 and 760 cm^{-1} in the 700–1200 cm^{-1} region. These Raman bands correspond to the surface molecularly dispersed vanadium oxide species.[41] No Raman bands of bulk V_2O_5 are observed. The H_2-TPR shown in Figure 2 reveals a single reduction peak at 767 K, with H/V ratio of 2.0 corresponding to V^{+5} to V^{+3} reduction. These results are consistent with previous studies indicating that reducible surface vanadium oxide species are present.[24,42] Furthermore, the 5% V_2O_5/Al_2O_3 corresponds to a coverage of 0.37 based on a monolayer coverage of 7.35 V atm/nm^2. Under dehydrated conditions, two types of molecularly dispersed vanadium oxide species are present on oxide supports: a monomeric and a polymeric vanadia species. The monomeric species is present

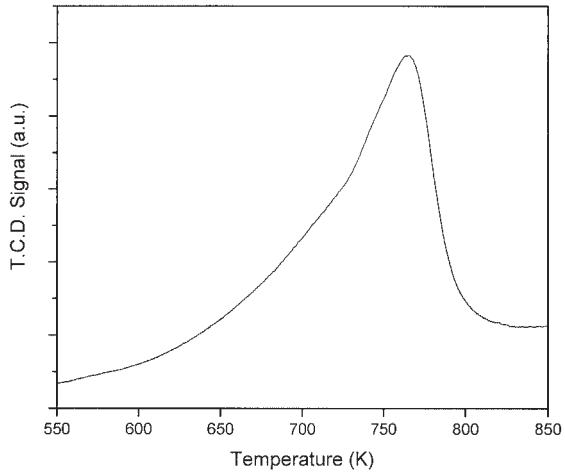

Figure 2. TPR profile of the catalyst.

as a major species at low coverages and polymeric species is present as a major species at high coverages.[42] For the 5% V_2O_5/Al_2O_3 sample it is expected that the monomeric vanadium oxide species is the dominant species.

Genetic algorithm model validation

To validate the application of GA as a means for estimating kinetic parameters, a multiresponse data set given by Box and Draper[12] is considered. The data set concerns a series reaction $A \rightarrow B \rightarrow C$. The mole fraction of the components A, B, and C, at anytime t can be expressed as

$$x_A = e^{-\phi_1 t}$$

$$x_B = (e^{-\phi_1 t} - e^{-\phi_2 t})\phi_1/(\phi_2 - \phi_1)$$

and

$$x_C = 1 + (-\phi_2 e^{-\phi_1 t} + \phi_1 e^{-\phi_2 t})/(\phi_2 - \phi_1) \qquad (27)$$

where, at anytime t, x_A, x_B, and x_C are the mole fractions of A, B, and C, respectively; and ϕ_1 and ϕ_2 are the unknown rate constants.

A determinant criterion described later is used for estimating the unknown rate constants in terms of ln ϕ_1 and ln ϕ_2. All 12 experiments performed by Box and Draper are used in the present study. The values of ln ϕ_1 and ln ϕ_2 are presented in Table 2 along with the kinetic parameter values determined by Box and Draper[12] and Kang and Bates,[34] who also used the same data set. The closeness of the kinetic parameter values obtained by Box and Draper[12] and Kang and Bates[34] and the present study suggests that using GA as a means to estimate kinetic parameters is comparable to, if not better than, methods used before.

Effect of GA parameters

The performance of GA depends on different GA parameters, such as the generation number, population size, crossover, and mutation probability. It is imperative to observe the convergence rate of the objective function with the change of these factors and its subsequent effect on the reliability of the kinetic parameters. The effect of the changes in GA parameter on the objective function or determinant value is shown in Figures 3a–3c. In these figures the values of the determinant obtained for the propane ODH over 5% V_2O_5/Al_2O_3 catalyst are plotted vs. the number of generations for different values of a GA parameter. From Figures 3a–3c it is observed that the determinant value rapidly decreases during the first 50 generations and then remains relatively constant. An increase in the number of generations > 200 has a negligible effect on the kinetic parameter and consumes a lot of computational time.

In Figure 3a the effect of population size on the decrease of the determinant value is observed. As the population size increases from 50 to 200 a stable determined value is quickly achieved. Furthermore, because of the spread of the solutions over the search space, with an increase in population size the chances of the determinant value converging to local optima decrease. The effects of crossover and mutation rates on the determinant values are presented in Figures 3b and 3c, respectively. From a comparison of the crossover and mutation rates from the figures it is observed that high crossover (0.8) and low mutation (0.2) rates are suitable for the application of GA in the present system because at other values truly optimum determinant values may not be achieved.

The GA parameters used in the present work are presented in Table 3. In addition to the above-discussed GA parameters, other parameters—such as tournament size and the exponents for simulated binary crossover and mutation—are also important. In the present study the tournament size is 2, and the exponents for simulated binary crossover and mutation are 2 and 200, respectively.

Reaction studies

Figure 4 shows the results of the contact-time studies carried out with the 5% V_2O_5/Al_2O_3 catalyst. The plot between the propane conversion and product selectivites vs. contact time provides useful insight into the reaction mechanism. It can be observed from Figure 4 that the conversion of propane increases with increasing contact time. The propene selectivity, however, decreases, whereas the CO and CO_2 selectivities increase with increasing contact time. These changes in product selectivities suggest that propene is a primary product and the carbon oxides are secondary products, results that are consistent with the present choice of a consecutive MVK reaction model.

The reaction data obtained for the second type of study are presented in Table 4. The data in the table are divided into three sets depending on the propane to oxygen ratio. In each set the data are arranged with increasing temperature. In the 1st and

Table 2. Kinetic Parameters of the Series Reaction Described by Box and Draper[12]

Parameter	Box and Draper[12]	Kang and Bates[34]	Present Study
θ_1	-1.570	-1.5723	-1.5775
θ_2	-0.707	-0.70222	-0.6636
Determinant value	3.145×10^{-6} *	3.134×10^{-6} *	3.045×10^{-6}

The determinant values are not given in the two papers cited and are calculated from the parameter values presented in the respective papers.

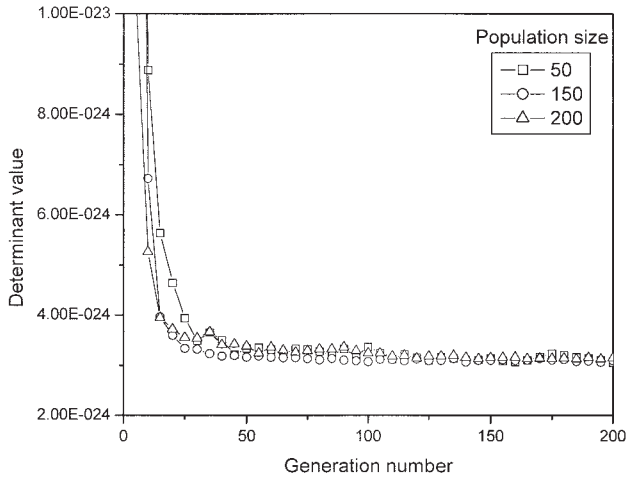

(a)

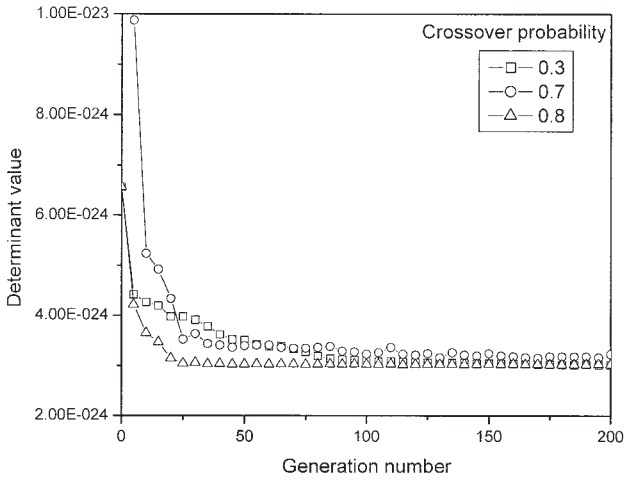

(b)

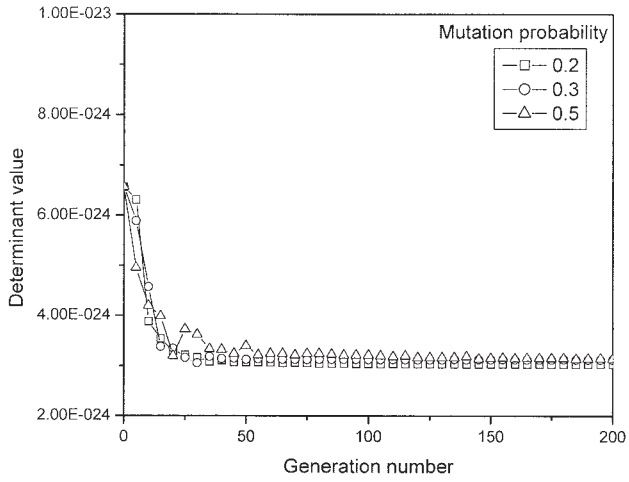

(c)

Figure 3. (a) Variation in determinant value with number of generations for different population size; (b) variation in determinant value with number of generations for different crossover probability; (c) variation in determinant value with number of generations for different mutation probability.

2nd columns the propane to oxygen ratio and the temperature at which the reactions carried out are provided. The yields of the products C_3H_6 and CO_x are shown in the 3rd and 4th columns, respectively. The C_{out}/C_{in} ratio is present in the last column of the table and indicates the accuracy of the GC measurements, which is within acceptable limits. From the table it is observed that at all propane to oxygen molar ratios the propene and CO_x yields increase with temperature. Furthermore, the ratio of CO to CO_2 in the outlet was about 1.4 and was practically independent of temperature and C_3H_8 to O_2

Table 3. GA Parameter Values Used in the Present Study

GA Parameter	Value
Generations (G_m)	200
Population size	200
Crossover probability	0.8
Mutation probability	0.2
Tournament size	2
Exponent for simulated binary crossover*	2
Exponent for mutation*	200

Used in the present GA and explained elsewhere.[10]

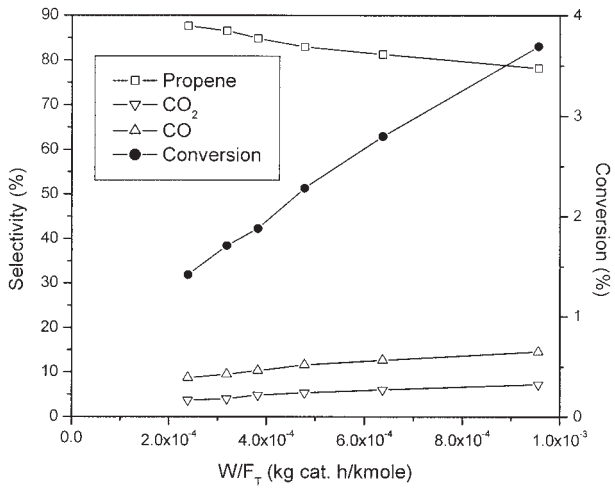

Figure 4. Variation of conversion and selectivity with contact time for propane ODH over 5% V_2O_5/Al_2O_3 catalyst.

C_3H_8:O_2 = 2:1, T = 713 K, Weight of the catalyst = 0.02 g.

Table 4. Reaction Studies for 5% V_2O_5/Al_2O_3 Catalyst Weight of the Catalyst = 0.2 gm; Total Flow Rate = 50 ml/min

C_3H_8:O_2 Molar Ratio	Temperature (K)	Yield (%)		C-Balance (C_{out}/C_{in})
		C_3H_6	CO_x	
1:1	673	1.32	0.81	1.01
	693	2.07	1.79	1.00
	713	3.05	3.57	0.99
	733	4.15	6.34	0.96
2:1	693	2.37	1.25	0.98
	713	3.92	3.01	1.03
	733	5.34	6.52	1.02
3:1	693	1.99	1.04	0.99
	713	3.00	2.35	0.96
	733	4.37	4.68	0.94

molar ratios. This value of Ψ was used for parameter estimation.

Parameter estimation

The kinetic parameters for the Mars–van Krevelen mechanism described earlier are estimated using a determinant criterion. The chosen MVK mechanism was found to be statistically adequate. When attempts were made to calculate the kinetic parameters without temperature centering, absurd values of preexponential factor and activation energies were obtained. When the temperature is noncentered in the Arrhenius equation for the estimation of kinetic parameter, unrealistic preexponential factor values have been previously observed.[29] Thus, temperature centering about the mean temperature helped to obtain realistic kinetic parameters.

The values of the kinetic parameters and their standard errors are presented in Table 5 along with their 90% likelihood intervals for nonlinear systems. The values of the standard error and likelihood intervals given in Table 5 suggest that the estimates of the kinetic parameters are reasonable. From the kinetic parameter values given in Table 5 it is observed that the preexponential factor for the ODH reaction is smaller by one order of magnitude than that for the combustion of propene to carbon oxides. The preexponential factor for reoxidation possesses an intermediate value. With respect to E_i values the activation energy for CO_x formation, E_2, is less than that for propene formation, E_1. The activation energy for the reoxidation of the catalyst, E_3, has a high value of 232 kJ/mol.

Similar trends in E_i values are observed for the activation energy for propene formation, E_1, and CO_x formation, E_2, by Argyle et al.[43] for a pseudo-first-order reaction scheme. They have shown that for propane ODH over V_2O_5/Al_2O_3 catalysts

Table 5. Kinetic Parameters, Their Standard Errors, and 90% Likelihood Interval for the MVK Model

Parameter* (Unit)	Value*	Standard Error	90% Likelihood Interval
k_{10} (min g cat^{-1})	16	1	(15, 17)
k_{20} (min g cat^{-1})	176	4	(173, 179)
k_{30} (min g cat^{-1})	68	4	(63, 72)
E_1 (kJ/mol)	123	6	(116, 132)
E_2 (kJ/mol)	58	14	(32, 84)
E_3 (kJ/mol)	232	20	(202, 264)

The parameters values are calculated at a T_m of 713.16 K.

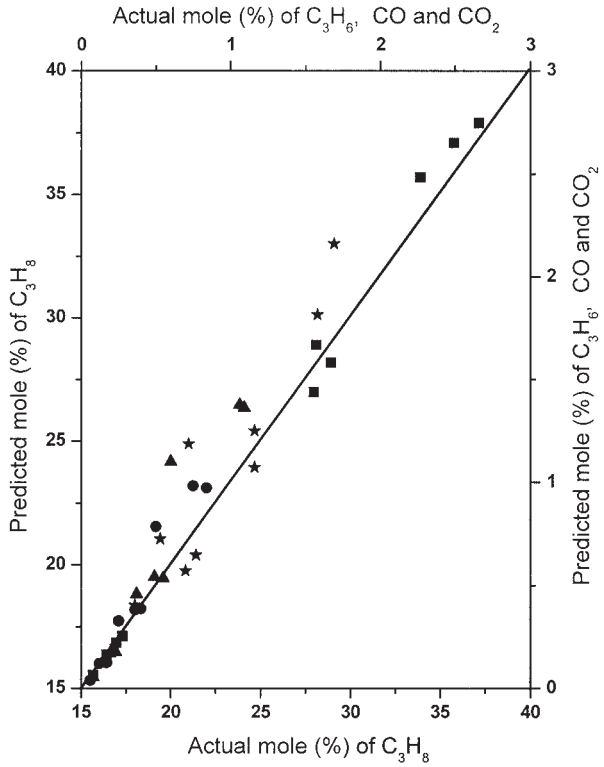

Figure 5. Comparison between the predicted and actual mole percentages of C_3H_8 (■), C_3H_6 (⋆), CO_2 (▲), and CO (●).

the activation energy for propene formation is greater than that for CO_x formation and range from 100 to 120 kJ/mol for the former and from 80 to 120 kJ/mol for the latter. For the propane ODH over a V-Mg-O catalyst using the MVK reaction model the activation energies for propene and CO_x formation were 75.5 and 64 kJ/mol, respectively.[13] Furthermore, the activation energy of reoxidation, E_3, for the V-Mg-O catalyst was 290 kJ/mol compared to 232 kJ/mol for the 5% V_2O_5/Al_2O_3 catalyst determined here. The reaction temperatures used for propane ODH over V-Mg-O catalyst are, however, different.

Using the kinetic parameters given in Table 5 the predicted outlet mole percentages of C_3H_8, C_3H_6, and CO_x are calculated and plotted vs. all the actual outlet mole percentages in Figure 5. The actual outlet mole percentages ranged from 15.65 to 37.15 for C_3H_8; from 0.23 to 1.69 for C_3H_6; from 0.08 to 1.09 for CO_2; and from 0.06 to 0.84 for CO. From Figure 5, the closeness of the predicted and actual concentrations is evident. However, care should be taken to interpret Figure 5 because only the sum of squares is represented, which is only a part of the determinant criteria used. As mentioned earlier the least-square optimization is ideally suitable for single-response systems and not for multiresponse nonlinear systems.

Profile plots

The profiling technique provides valuable information about the nonlinear nature of the parameters, the correlation among them, likelihood intervals of the parameters, and any reparameterization required. The profile t plots of τ vs. δ for all the

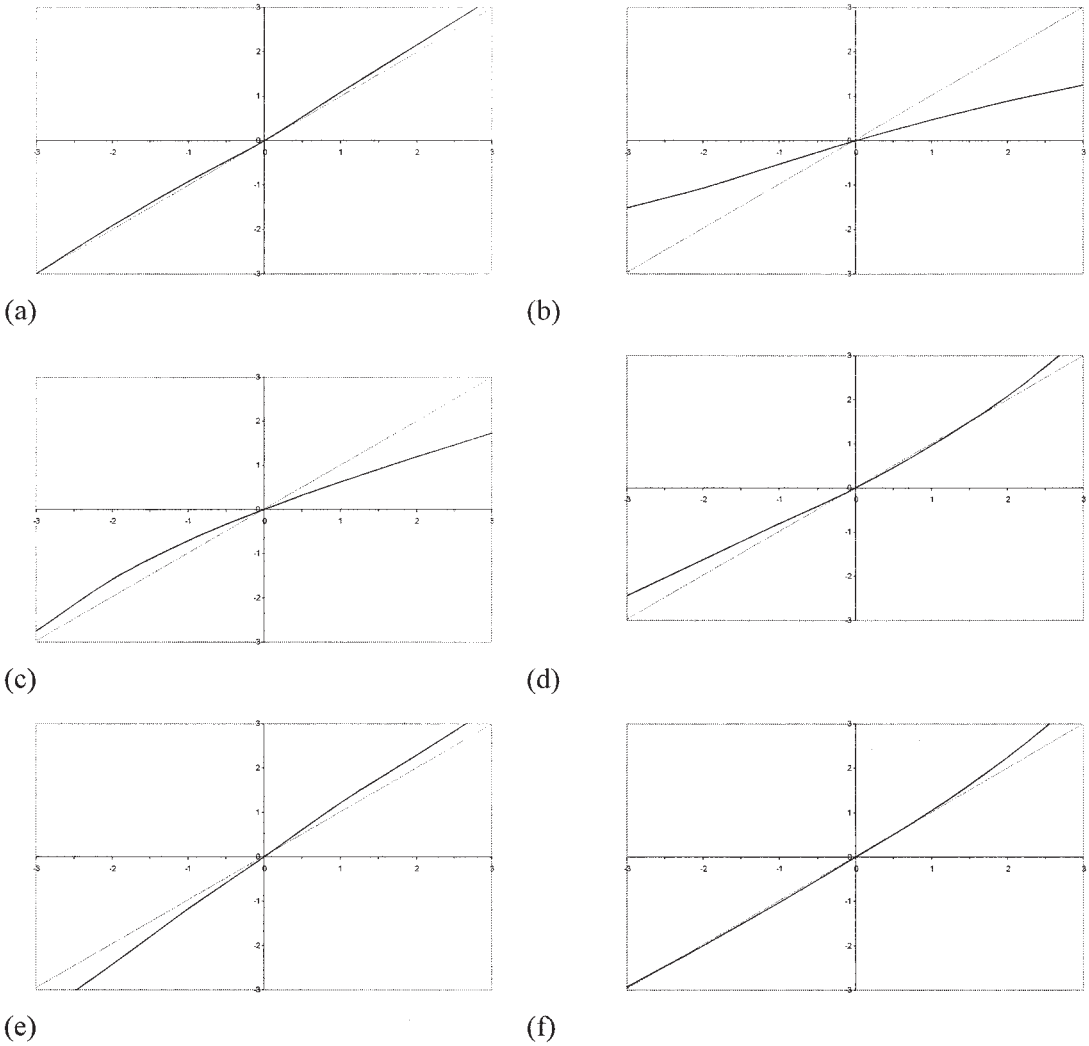

Figure 6. Profile *t* plots for (a) $\tau(k_{10})$ vs. $\delta(k_{10})$, (b) $\tau(k_{20})$ vs. $\delta(k_{20})$, (c) $\tau(k_{30})$ vs. $\delta(k_{30})$, (d) $\tau(E_1)$ vs. $\delta(E_1)$, (e) $\tau(E_2)$ vs. $\delta(E_2)$, and (f) $\tau(E_3)$ vs. $\delta(E_3)$.

The scale for both axis is from −3 to +3 with an increment of 1.

parameters are generated to analyze their extent of nonlinearity. The deviation of the plots from a straight line passing through the origin with unit slope reveals the degree of nonlinearity with respect to that parameter. For example, the profile t plot of k_{10} is shown in Figure 6a and it almost coincides with the straight line passing through the origin with unit slope, which is indicated by a dashed line. The coincidence of the two lines suggests that the nonlinearity with respect to k_{10} is practically nonexistent. Different degrees of nonlinearity are observed for the remaining parameters from their respective profile t plots (Figures 6b–6f). Specifically, the nonlinearity is more pronounced for k_{20} and k_{30} than that for E_1, E_2, and E_3. The two parameters k_{20} and k_{30} are associated with formation of carbon oxides and reoxidation of the oxide support, respectively. The presence of nonlinearity in k_{20} and k_{30} may be associated with the lumping together of different reaction pathways into a single reaction step. For example, the CO and CO_2 formation is lumped together in a single reaction step r_2 possessing a preexponential factor of k_{20} and activation energy of E_2; and the different reoxidation mechanisms have been lumped together by a single mechanism with a preexponential factor of k_{30} and activation energy E_3. Different pathways for the formation of CO, CO_2,[44] and for reoxidation have been previously observed.[45] It is observed that delumping of r_2 into separate steps for CO and CO_2 formation indeed decreases the nonlinearity associated with k_{20}. It appears that further delumping of the reaction pathways would reduce the nonlinearity, although the number of kinetic parameters required to describe the reaction model would increase. The increase in the number of parameters would require additional experiments to be conducted.

The profile trace plots provide information about the correlation between two parameters. The absence of correlation between two parameters θ_p and θ_q is confirmed if the plots of $\tilde{\delta}(\theta_q)$ vs. $\delta(\theta_p)$ and $\tilde{\delta}(\theta_p)$ vs. $\delta(\theta_q)$ intersect each other at 90°. For nonlinear models, the profile trace plots will be curved if correlation between parameters exists. For the six parameters of the MVK model there are 15 profile trace plots, of which a few representative ones are shown in Figures 7a–7f and discussed.

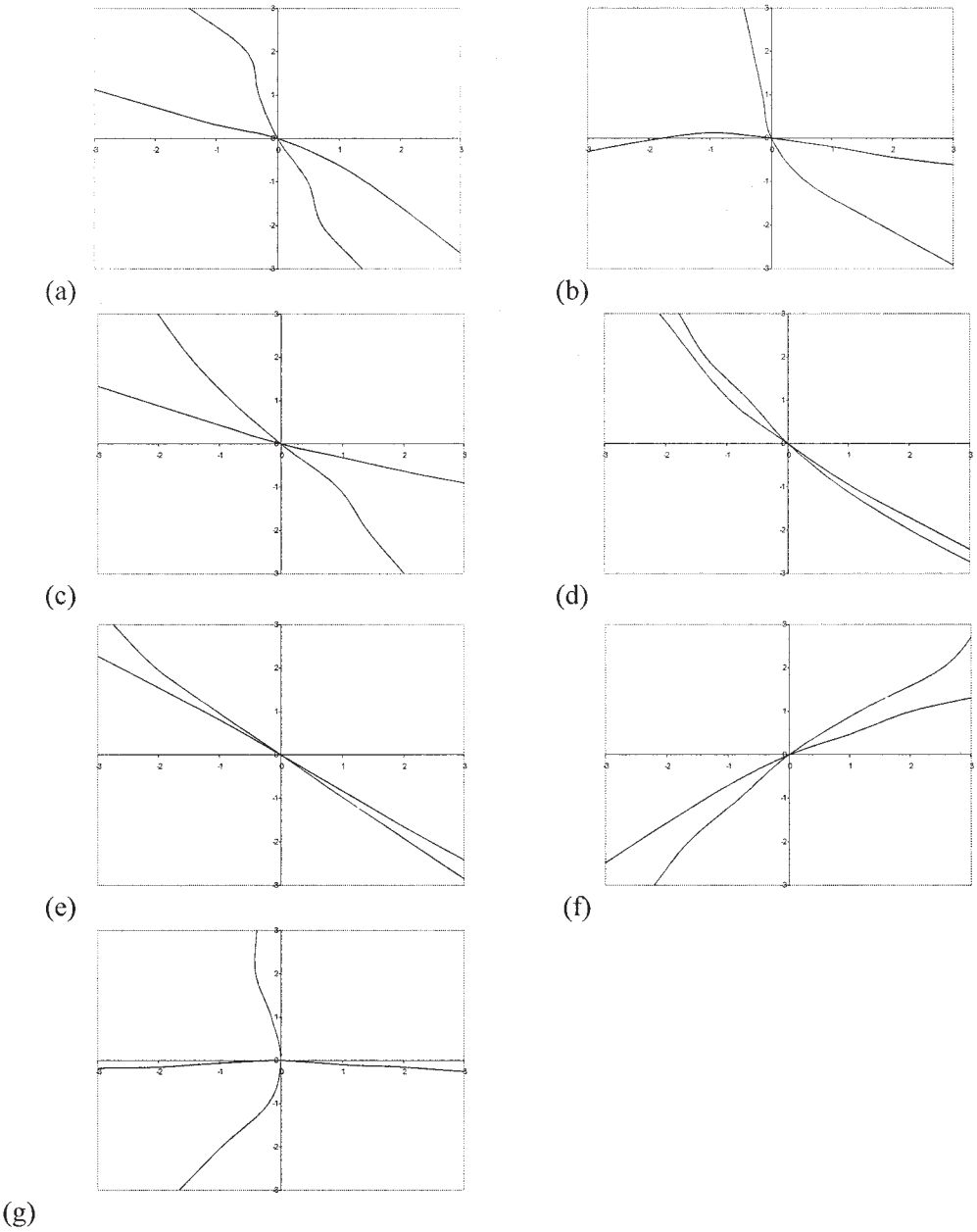

Figure 7. Selected profile trace plots (a) $\delta(E_1)$ vs. $\delta(k_{10})$, (b) $\delta(E_2)$ vs. $\delta(k_{20})$, (c) $\delta(E_3)$ vs. $\delta(k_{30})$, (d) $\delta(k_{30})$ vs. $\delta(k_{20})$, (e) $\delta(E_1)$ vs. $\delta(k_{20})$, (f) $\delta(E_1)$ vs. $\delta(k_{30})$, and (g) $\delta(E_2)$ vs. $\delta(k_{30})$.

The scale for both axis is from -3 to $+3$ with an increment of 1.

It is observed that the profile trace plots between E_1 vs. k_{10}, E_2 vs. k_{20}, and E_3 vs. k_{30} in Figures 7a–7c do not intersect at acute angles, which suggests that the centering technique helped to linearize the Arrhenius parameters. Complete elimination of correlations between the Arrhenius parameters, however, is not achieved. Similar profile trace plots are observed between k_{10} and k_{20}, k_{10} and k_{30}, and k_{30} and E_2, suggesting that the correlation between these kinetic parameters is not completely eliminated. In contrast, almost coincidental profile trace plots in Figures 7d–7f show the robust parameter correlation between k_{20}, k_{30}, and E_1. Robust parameter correlation is also observed between E_2 and E_3. Less rigorous correlations are observed between k_{10} and E_2, k_{10} and E_3, k_{20} and E_3, E_1 and E_2, and E_1 and E_3. For the sake of brevity the profile traces for these parameters are not shown. Thus, estimations of parameters and the corresponding profile t and trace plots for the present study reveal that nonlinearity and correlations between parameters exist. Centering has helped in reducing the nonlinearity; however, correlations between parameters still exist and other methods to remove correlation between parameters should be considered. Furthermore, application of linear approximation is not recommended because the nonlinearity is present even after temperature centering.

The estimated kinetic parameters can be used for revealing

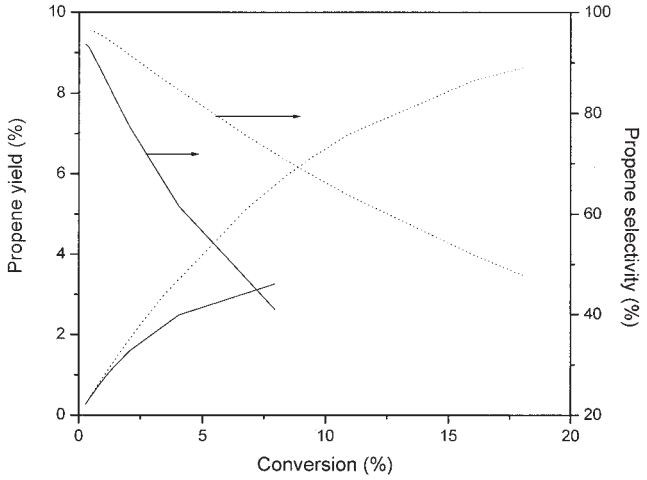

Figure 8. Variation in propene yield and selectivity with conversion at 663 K (—) and 733 K (- - -) for 5% V_2O_5/Al_2O_3 catalyst.

$C_3H_8:O_2 = 2:1$.

more about the reaction, for operating the reactor under optimized conditions, and for catalyst design. For example, from the values of the preexponential factors, k_{i0}, and activation energies, E_i, of propene and CO_x formation, the variation of propene yield and selectivity with fractional conversion can be calculated. This variation is shown in Figure 8 for propane to oxygen ratio of 2:1 at two temperatures, 663 and 733 K. The figure reveals that the propene yield increases and the propene selectivity decreases with an increase in fractional conversion for both temperatures. Furthermore, at a particular conversion the propene yield and propene selectivity increases with increasing temperature. With an increase in temperature the ratio of k_2/k_1 decreases, which is attributed to the difference between the activation energies E_2 and E_1, $(E_2 - E_1)$. For first-order consecutive reactions the propene yield also increases with conversion.[20] At a particular conversion the propene yield and selectivity also increases with an increase in temperature. Although a first-order reaction is not entirely valid here, the trends in propene yield and propene selectivity with k_2/k_1 ratio are similar for the first-order consecutive reaction and the present study.

In the present study determining optimum contact times for maximizing propene yield was not possible because the oxygen becomes the limiting reactant and is consumed before optimum contact times can be reached. Therefore, for obtaining optimum contact times the propane to oxygen ratio should be such that oxygen is present in excess. Assuming that the kinetic parameters can be extrapolated to conditions beyond those used in the present study (such as a propane to oxygen ratio of 1:10), the optimum propene yields and the corresponding conversions are determined for various temperatures and, consequently, different k_2/k_1 ratios. The values of the optimum propene yield and the corresponding conversions are plotted vs. k_2/k_1 ratio in Figure 9. Included in Figure 9 are the curves obtained for a first-order consecutive reaction based on the formulae given by Fogler.[20] The figure reveals that the optimum yield and the corresponding conversion decrease with an increase in k_2/k_1 value for the first-order consecutive reaction given by Fogler[20] and the present study. Furthermore, there is a close correspondence between the values obtained in the present study and those obtained for a first-order consecutive reaction. The MVK mechanism used in this study involves the factor β in addition to the other terms in Eqs. 19 and 20. For conditions of excess oxygen the β term does not change significantly and thus the reaction is pseudo first order. Considering that pseudo-first-order consecutive reactions are occurring it is not surprising that the optimum yield and the corresponding conversion in the present study for extrapolated conditions almost overlap those for consecutive first-order reactions in Fogler.[20]

Figure 8 reveals that propene yield increases with an increase in temperature corresponding to a decrease in k_2/k_1 value. Figure 9 shows that the optimum conditions can be achieved for different k_2/k_1 ratios. For lower k_2/k_1 values the optimum propene yield increases. In the present study increasing the reaction temperature decreases the k_2/k_1 ratio. In addition to decreasing the k_2/k_1 ratio by increasing the temperature a change in the catalyst can also affect changes in the k_2/k_1 ratio. The change in the catalyst essentially involves changing the chemical composition. By changing the catalyst composition the kinetic parameters k_{i0} and E_i change and the best catalyst will be that with the lowest k_{20}/k_{10} ratio and the maximum difference between E_2 and E_1. A combination of these two will provide a low k_2/k_1 value. Inherent in this analysis is that the same reaction mechanism is valid. For more complicated reaction mechanisms appropriate modifications of the above statements regarding optimum propene yield are necessary. Thus, proper tuning of k_{10}, k_{20}, E_1, and E_2 will assist in obtaining a good catalyst for propane ODH.

In summary, proper characterization of the catalyst is required for the development of a suitable reaction mechanism. Based on the reaction mechanism the kinetic parameters can be estimated based on a suitable estimation criterion and tested for their nonlinearity and correlations. Using the estimated kinetic parameters the appropriate operating conditions can be specified and the reaction mechanism can be better understood. Furthermore, the kinetic parameters can be used for catalyst design. With an appropriate choice of the chemical composi-

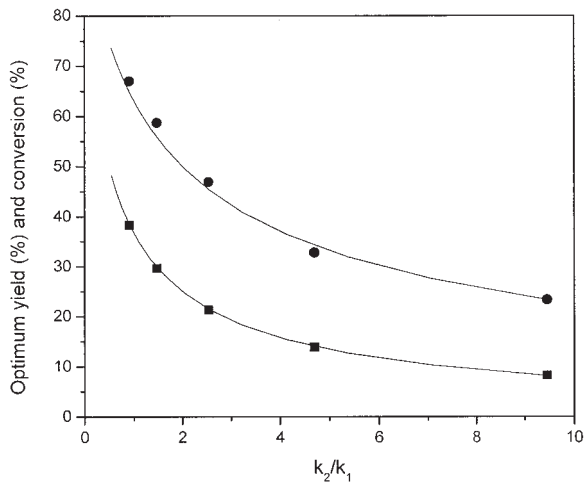

Figure 9. Variation in optimum yield (■) and conversion (●) with k_2/k_1 ratio and comparison with first-order consecutive reaction (lines).

tion and/or temperature, necessary changes in the kinetic parameters can be obtained.

Conclusion

A 5% V_2O_5/Al_2O_3 catalyst was synthesized using the incipient-wetness impregnation technique and tested for the propane ODH reaction for which the steady-state kinetic parameters are estimated. Initially, the 5% V_2O_5/Al_2O_3 catalyst was characterized to determine the nature of the vanadium oxide species and its effect on the support. It was observed that surface vanadium oxide species are formed and the Al_2O_3 support is unaffected. Furthermore, the surface vanadium oxide species shows expected reduction behavior with a T_{max} during reduction at 767 K and H/V value of 2 corresponding to a reduction from V^{+5} to V^{+3}. Reaction data suggest that the CO_x's (CO and CO_2) were essentially formed as secondary products. Consequently, the choice of a single-site consecutive Mars–van Krevelen mechanism appears justified. Based on steady-state reaction data obtained at different C_3H_8:O_2 ratios and temperatures the kinetic parameters were estimated using nonlinear multiresponse analysis. A determinant criterion was chosen as the objective function to be minimized. The minimization was achieved with the help of a real-coded GA with appropriate choice of GA parameters. The kinetic parameters obtained after minimization was then tested using a profiling technique. The profiling technique provides information on the nonlinearity of the parameter and model, correlation between parameters, and maximum likelihood intervals. By using the kinetic parameters it is then possible to better understand the reaction, optimize reaction conditions, if possible, and use it for a better catalyst design.

Acknowledgments

The authors are grateful to the Ministry of Human Resource and Development (MHRD), India for partial financial support.

Notation

c = concentration of reactant, mol/cm^3
c_i = concentration of reactant i, mol/cm^3
$C_{C_3H_8B}$ = bulk concentration of propane, mol/m^3
$C_{C_3H_8S}$ = concentration of propane at the external surface of the catalyst particle, mol/m^3
d = determinant value
d_p = diameter of catalyst particle, m
D_e = effective diffusion coefficient, m^2/s
D_r = radial diffusivity, cm^2/s
E = true activation energy, kJ/mol
E_i = activation energy for the reaction, kJ/mol
$g_i(X_u, \theta)$ = expected value of response i for uth experiment
$F_{P,N-P;\alpha}$ = F distribution with P and $N - P$ degrees of freedom at upper α quantile
F_T = total flow rate, cm^3/min
G_N = number of generations
G_{Nm} = maximum number of generations
h = heat transfer coefficient, kJ h^{-1} m^{-2} cat^{-1} K^{-1}
ΔH = heat of chemical reaction, kJ/mol
k_c = gas-particle mass transfer coefficient, m/s
k_j = rate constant for the reaction jth reaction
k_{io} = preexponential factor
n = order of reaction
N = number of experiments
P = number of parameters
P_i = partial pressure of the component i
P_T = total pressure of the system, Pa
r = radial position, m
$-r'_{C_3H_8}$ (obs) = measured rate of reaction, mol (kg catalyst)$^{-1}$ s^{-1}
r_p = catalyst particle radius, m
R = gas constant, kJ kmol^{-1} K^{-1}
Re = Reynolds number
R_{pi} = reaction rate for component i, Pa s^{-1} (g of catalyst)$^{-1}$
R_v = reaction rate, mol s^{-1} cm^{-3}
R_w = reaction rate, mol s^{-1} (g of catalyst)$^{-1}$
R_{wi} = reaction rate for component i, mol/s-g of catalyst
sgn = sign function: $\text{sgn}(\theta_P - \hat{\theta}_P) = -1$, $(\theta_P - \hat{\theta}_P) < 0$; $sgn(\theta_P - \hat{\theta}_P) = 0$, $(\theta_P - \hat{\theta}_P) = 0$; $sgn(\theta_P - \hat{\theta}_P) = +1$, $(\theta_P - \hat{\theta}_P) > 0$
se = parameter standard error
s^2 = scale factor
S = sum of square
T = actual reaction temperature, K
T_s = temperature at the catalyst surface, K
T_m = mean temperature, K
u = interstitial velocity, m/s
W = weight of the catalyst, g
x_i = mole fraction of component i at any time
X_i = inlet mole fraction of component i
X_u = vector of experimental variables (that is, inlet mole fractions of propane, oxygen, and temperature) for uth experiment
y_{ui} = response variable i for uth experiment
$\mathbf{Y}$ = vector of variables representing the response
z = axial distance, m
z_{ui} = error associated with the response i for uth experiment
$\mathbf{Z}$ = error vector

Greek letters

α = significance level
β = degree of reduction of the catalyst
$\delta(\theta_P)$ = studentized value of parameter θ_p
$\tau(\theta_P)$ = profile t value for parameter θ_P
θ = parameter vectors
λ = thermal conductivity of the particle, W m^{-1} K^{-1}
Ψ = ratio between the number of moles of CO_2 to CO
ν = kinematic viscosity, m^2/s
ε = 1 for CO, 2 for CO_2
ρ_b = bulk density of the catalyst bed, kg catalyst/m^3
$\mathbf{\Gamma}$ = Hessian matrix
σ = contact time, s

Subscripts

i = component
p = catalyst particle
pp = diagonal element
u = experiment number

Superscripts

^ = estimates
~ = conditional minimum value

Literature Cited

1. Boudart M, Djega-Mariadassou G. *Kinetics of Heterogeneous Catalytic Reactions*. 1st Edition. Princeton, NJ: Princeton Univ. Press; 1984.
2. Carberry JJ. Designing laboratory catalytic reactors. *Ind Eng Chem*. 1964;56:39-44.
3. Froment GF. Model discrimination and parameter estimation in heterogeneous catalysis. *AIChE J*. 1975;21:1041-1057.
4. Mears DE. Tests for transport limitations in experimental catalytic reactors. *Ind Eng Chem Proc Des Dev*. 1971;10:541-547.
5. Bates DM, Watts DG. A generalized Gauss–Newton procedure for multiresponse parameter estimation. *SIAM J Sci Stat Comput*. 1987; 8:49-55.
6. Moros R, Kalies H, Rex HG, Schaffarczyk ST. A genetic algorithm for

generating initial parameter estimations for kinetic models for catalytic processes. *Comput Chem Eng*. 1996;20:1257-1270.
7. Park T-Y, Froment GF. A hybrid genetic algorithm for the estimation of parameters in detailed kinetic models. *Comput Chem Eng*. 1998; 22:103-110.
8. Wolf D, Moros R. Estimating rate constants of heterogeneous catalytic reactions without supposition of rate determining surface steps—An application of a genetic algorithm. *Chem Eng Sci*. 1997;52:1189-1199.
9. Edwards K, Edgar TF, Manousiouthakis VI. Kinetic model reduction using genetic algorithm. *Comput Chem Eng*. 1998;22:239-246.
10. Deb K. *Multi-Objective Optimization Using Evolutionary Algorithms*. 1st Edition. London: Wiley; 2002.
11. Deb K. *Optimization for Engineering Design: Algorithms and Examples*. 1st Edition. New Delhi, India: Prentice-Hall of India Private Ltd; 1998.
12. Box GEP, Draper NR. The Bayesian estimation of common parameters from several responses. *Biometrika*. 1965;52:355-365.
13. Creaser D, Andersson B. Oxidative dehydrogenation of propane over V-Mg-O: Kinetic investigation by nonlinear regression analysis. *Appl Catal A Gen*. 1996;141:131-152.
14. Grabowski R, Sloczyñski J, Grzesik NM. Kinetics of oxidative dehydrogenation of propane over V_2O_5/TiO_2 catalyst. *Appl Catal A Gen*. 2003;242:297-309.
15. Bates DM, Watts DG. *Nonlinear Regression Analysis and Its Applications*. 1st Edition. New York, NY: Wiley; 1988.
16. Kung HH. Oxidative dehydrogenation of light (C2 to C4) alkanes. *Adv Catal*. 1994;40:1-38.
17. International Editorial Board, ed. Industrial inorganic chemicals and products. *An Ullmann's Encyclopedia*. Weinheim, Germany: Wiley–VCH; 1999.
18. Cherian M, Rao MS, Yang WT, Jehng J-M, Hirt AM, Deo G. Oxidative dehydrogenation of propane over Cr_2O_3/Al_2O_3 and Cr_2O_3 catalysts: Effects of loading, precursor and surface area. *Appl Catal A Gen*. 2002;233:21-32.
19. Kanpur Genetic Algorithm Lab (KanGAL), India. http://www.iitk.ac.in/kangal/soft.htm
20. Fogler HS. *Elements of Chemical Reaction Engineering*. 2nd Edition. New Delhi, India: Prentice-Hall of India Private Ltd; 2001.
21. Bottiono A, Capabnnelli G, Comite A, Storace S, Felice RD. Kinetic investigation on the oxidehydrogenation of propane over vanadium supported on γ-Al_2O_3. *Chem Eng J*. 2003;94:11-18.
22. Andersson SLT. Kinetic study of the oxidative dehydrogenation of propane over vanadia supported on amorphous $AlPO_4$. *Appl Catal A Gen*. 1994;112:209-218.
23. Stern DL, Grasselli RK. Reaction network and kinetics of propane oxydehydrogenation over nickel cobalt molybdate. *J Catal*. 1997;167: 560-569.
24. Routray K, Reddy KRSK, Deo G. Oxidative dehydrogenation of propane on V_2O_5/Al_2O_3 and V_2O_5/TiO_2 catalysts: Understanding the effect of support by parameter estimation. *Appl Catal A Gen*. 2004; 265:103-113.
25. Baldi M, Finocchio E, Pistarino C, Busca G. Evaluation of the mechanism of the oxy-dehydrogenation of propane over manganese oxide. *Appl Catal A Gen*. 1998;173:61-74.
26. Pritchard DJ, Bacon DW. Prospects of reducing correlation among parameters estimates in kinetic models. *Chem Eng Sci*. 1978;33:1539-1543.
27. Brauner N, Shacham M. Statistical analysis of linear and nonlinear correlation of the Arrhenius equation constants. *Chem Eng Process*. 1997;36:243-249.
28. McLean DD. Discussion. *Technometrics*. 1985;27:340-348.
29. Watts DG. Estimating parameters in nonlinear rate equations. *Can J Chem Eng*. 1994;72:701-710.
30. Hunter WG. Estimation of unknown constants from multiresponse data. *Ind Eng Chem Fundam*. 1967;6:461-463.
31. Mezaki R, Butt JB. Estimation of rate constants from multiresponse kinetic data. *Ind Eng Chem Fundam*. 1968;7:120-125.
32. McLean DD, Pritchard DJ, Bacon DW, Downie J. Singularities in multiresponse modelling. *Technometrics*. 1979;21:291-298.
33. Stewart WE, Sorensen JP. Bayesian estimation of common parameters from multiresponse data with missing observations. *Technometrics*. 1981;23:131-141.
34. Kang G, Bates DM. Approximate inferences in multiresponse regression analysis. *Biometrika*. 1990;77:321-331.
35. Stewart WE, Caracotsios M, Sorenson JP. Parameter estimation from multiresponse data. *AIChE J*. 1992;38:641-650.
36. Guay M, McLean DD. Optimization and sensitivity analysis for multiresponse parameter estimation in systems of ordinary differential equations. *Comput Chem Eng*. 1995;9:1271-1285.
37. Ertl G, Knozinger H, Weitkamp J, eds. *Handbook of Heterogeneous Catalysis*. Weinheim, Germany: VCH; 1997.
38. Soo YW, Bates DM. Multiresponse spline regression. *Comput Stat Data An*. 1996;22:619-631.
39. Box GEP, Hunter WG, MacGregor JF, Erjavec J. Some problems associated with the analysis of multiresponse data. *Technometrics*. 1973;15:33-51.
40. Bates DM, Watts DG. Multiresponse estimation with special application to linear systems of differential equations. *Technometrics*. 1985; 27:329-339.
41. Deo G, Wachs IE. Predicting the molecular structures of surface metal oxide species on oxide supports under ambient conditions. *J Phys Chem*. 1991;95:5889-5901.
42. Deo G, Wachs IE, Haber J. Supported vanadium oxide catalysts: Molecular structural characterization and reactivity properties. *Crit Rev Surf Chem*. 1994;4:141-187.
43. Argyle MD, Chen K, Bell AT, Iglesia E. Effect of catalyst structure on oxidative dehydrogenation of ethane and propane on alumina-supported vanadia. *J Catal*. 2002;208:139-149.
44. Creaser DC, Andersson B, Hudgins RR, Silveston PL. Kinetic modelling of oxygen dependence in oxidation dehydrogenation of propane. *Can J Chem Eng*. 2000;78:182-193.
45. Doornkamp C, Clement M, Gao X, Deo G, Wachs IE, Ponec V. The oxygen isotopic exchange reaction on vanadium oxide catalysts. *J Catal*. 1999;185:415-422.

Manuscript received Apr. 1, 2004, and revision received Oct. 21, 2004.